Designing patient-oriented combination therapies for acute myeloid leukemia based on efficacy/toxicity integration and bipartite network modeling

Mehdi Mirzaie[a,†], Elham Gholizadeh[a,†], Juho J. Miettinen[b], Filipp Ianevski[b], Tanja Ruokoranta[b], Jani Saarela[b], MikkoManninen[c], Susanna Miettinen[d], Caroline A. Heckman[e,*], and Mohieddin Jafari[a,*]

[a]Department of Biochemistry and Developmental Biology, University of Helsinki, Helsinki, Finland; [b]Institute for Molecular Medicine Finland, Helsinki Institute of Life Science,University of Helsinki, Helsinki, Finland; [c]Orton Orthopaedic Hospital, Helsinki, Finland; [d]Adult Stem Cell Group, Faculty of Medicine and Health Technology, Tampere University, Tampere, Finland; [e]Institute for Molecular Medicine Finland - FIMM, HiLIFE - Helsinki Institute of Life Science, iCAN Digital Precision Cancer Medicine Flagship, University of Helsinki, Helsinki, Finland

Key Points

- Ruxolitinib-ulixertinib and sapanisertib-LY3009120 have the best synergistic effects on AML, with the least toxicity.
- This study's combinations destroy blasts without harming other healthy cells, unlike standard chemotherapy, which is less specific.

Abstract

Acute myeloid leukemia (AML), a heterogeneous and aggressive blood cancer, does not respond well to single-drug therapy. A combination of drugs is required to effectively treat this disease. Computational models are critical for combination therapy discovery due to the tens of thousands of two-drug combinations, even with approved drugs. While predicting synergistic drugs is the focus of current methods, few consider drug efficacy and potential toxicity, which are crucial for treatment success. To find effective new drug candidates, we constructed a bipartite network using patient-derived tumor samples and drugs. The network is based on drug-response screening and summarizes all treatment response heterogeneity as drug response weights. This bipartite network is then projected onto the drug part, resulting in the drug similarity network. Distinct drug clusters were identified using community detection methods, each targeting different biological processes and pathways as revealed by enrichment and pathway analysis of the drugs' protein targets. Four drugs with the highest efficacy and lowest toxicity from each cluster were selected and tested for drug sensitivity using cell viability assays on various samples. Results show that the combinations of ruxolitinib-ulixertinib and sapanisertib-LY3009120 are the most effective with the least toxicity and best synergistic effects on blasts. These findings lay the foundation for personalized and successful AML therapies, ultimately leading to the development of drug combinations that can be used alongside standard first-line AML treatment.

Keywords: Drug combination design; Acute myeloid leukemia (AML); Nominal data mining; Bipartite network modeling; High-throughput drug screening; drug efficacy; drug toxicity

Introduction

Acute myeloid leukemia (AML) is an inter- and intra-tumor heterogeneous disease [1,2]. It is identified when the bone marrow (BM) contains at least 20% of blast cells of the myeloid lineage [3]. Traditional chemotherapeutics have limited efficacy in patients over the age of 65, with a survival rate of less than 25% at one year follow-up and less than 9% after 5 years [4]. Despite recent advances in genome sequencing, which enables researchers to identify a large number of mutations, we are still hampered by the absence of drugs which specifically target cancer-associated mutations [5]. On the other hand, the majority of AML patients do not have actionable mutations, and the link between cancer genotype, phenotype, and therapeutic function is poorly understood [6]. Even if we overcome the above difficulties and identify the exact mutations in genotype, monotherapy drug resistance will remain a major clinical complication [7]. Targeted anti-cancer compounds used in combination therapy have the potential to overcome resistance, improve patient response to current treatments, reduce dose-limiting single agent toxicity, and broaden the spectrum of available therapies [8].

Drug combination therapy offers the chance to suppress a number of pathways synergistically, including patient-specific cancer rescue pathways and phenotypic redundancy across heterogeneous cancer sub-clones [9]. The phenotypic effects of thousands of drug combinations can be evaluated in patient-derived cells and other pre-clinical model systems using high-throughput screening. However, because there are so many possible drug and dose combinations, large-scale multi-dose combinatorial screening is not recommended, due to the limited number of cells available from patient samples. Using the presented method in this study, researchers would be able to categorize the most important AML drugs into different clusters, each of which target proteins associated with various signaling pathways.

In our earlier research, we designed a systems pharmacology approach based on network

modeling to identify prospective drug combinations in AML [10]. To gain a deeper understanding of the factors that govern drug response in AML patients, we utilized a unique and extensive dataset obtained through drug response screening of samples from both AML patients and healthy donors in Finland as part of our study. Our model accounts for the efficacy and toxicity of drug response, which are simultaneously evaluated on patient and healthy samples, respectively [11]. A weighted bipartite network composed of two parts, chemical components, and patient samples was built to develop a drug combination strategy using the screening outcomes of single drug responses on AML patient samples. This enables researchers to directly access the phenotype of the patients' cancer cells through *ex vivo* drug response data, and by using network modeling and clustering analysis, demonstrate the drugs functionalities. Next, top drug combinations can be predicted based on phenotypic responses of samples in each cluster. In addition, we used two different computational resources, i.e., molecular biology annotations, and the chemical structure of drugs, to perform intra-cluster homogeneity analysis. The top combinations for further study in current pre-clinical drug combination screening are frequently chosen based on synergy alone, without taking into account the combination efficacy and toxicity effects, despite the fact that these are critical determinants of a therapy's clinical success [12].

Considering the importance of toxicity, in this study, we investigated the drug response of AML patient and healthy donor samples to calculate both efficacy and toxicity, respectively. The efficacy and toxicity of the drugs was assessed *ex vivo* on AML patient samples using cell viability and flow cytometry assays. Since clinical symptoms in patients are caused by blast cell accumulation in bone marrow [13], based on the assessment of CD marker expressions, we suggested the most blast-specific combinations as promising combinations for AML treatment. The novel combinations indicated in this study are effective on blasts but have a reduced level of toxicity on other cell populations, whereas with standard

chemotherapy the majority of the blasts are killed together with other cell types.

Results

The entire workflow of this study is depicted in Figure 1 and detailed material and method is presented in the supplementary information. The drug responses of 525 chemical compound tested on 199 AML patients' bone marrow samples were obtained from the FIMM AML data set[11]. The bipartite network was constructed using this data set, as explained in the materials and methods section in the supplement. A bipartite network can be projected into two different types of unipartite networks containing nodes of only one type. The projection of the bipartite network, onto the "drug" node set is considered here, called the drug similarity network. The Louvain community detection approach was used to find drugs that behaved similarly in terms of drug response[14]. The results gave us two communities (clusters) of drugs denoted by C_1 and C_2 with network sizes of 155 and 141, respectively (Table S1).

Comparing AML drug clusters: Evaluating protein target pathways and chemical structure similarity

We used two independent computational methods to determine how distinct the two clusters are: the first identifies the significant difference between biological pathways of drug protein targets in each cluster, and the second evaluates the chemical structure similarity of drugs in each cluster. We constructed a drug-target network using the drug target commons (DTC) database[15], which is also a bipartite network in which each link connects drugs to their protein targets. Let T_1 and T_2 represent the set of protein targets of drugs in the cluster C_1 and C_2, respectively, and T represents the union of $T_1$and T_2. In this study $|T_1| = 921, |T_2| = 842, and\ |T| = 1055.$

Proteins with a score S (explained in the supplementary information 1.3) greater than log (2) are considered to be preferentially targeted by drugs in cluster 1, denoted by PPT1. Similarly, PPT2 proteins have a score of less than $log(0.50)$. We performed GSEA (gene

set enrichment analysis) on PPT1 and PPT2 proteins based on their associated scoring functions. As expected, the biological processes and signaling pathways affected by drugs in Clusters 1 and 2 are distinct. This difference enables us to inhibit two different signaling pathways using one combination. Drugs in cluster 1 (PPT1), such as LY3009120 (a Pan-RAF inhibitor), predominantly target proteins associated with the RAF-MEK-ERK signaling pathway. This pathway plays a crucial role in cell proliferation and growth, indirectly influencing processes like cell-substrate adhesion and ion trans-membrane transport, which are enriched in our analysis [16]. In contrast, JAK1/2 inhibitors like ruxolitinib target JAK proteins, involved in cytokine signaling and immune responses, impacting pathways related to neuroactive ligand-receptor interactions and the regulation of actin cytoskeleton [17]. Drugs like birabresib, which target proteins in the bromodomain and extra-terminal (BET) family, have a role in gene regulation through chromatin binding, affecting gene expression and pathways related to chemical reactions and collagen metabolism [18]. Plicamycin, which binds to guanine-cytosine-rich regions of DNA, may influence gene expression and regulation, impacting pathways related to collagen metabolism and other DNA-dependent processes (Figure 2 A) [19]. On the other hand, proteins targeted by drugs in cluster 2 (PPT2) (silmitasertib, ulixertinib, sapanisertib, and teniposide) are in the p53 signaling pathway, cell cycle, apoptosis, and pancreatic, colorectal and chronic myeloid leukemia cancers and related to tumorigenesis and progression pathways, including human immunodeficiency virus 1 infection [20-23].

We also performed ShinyGO [24] Gene Ontology and KEGG pathway enrichment analysis on proteins that are merely targeted by drugs in one cluster. For this purpose, two protein sets G1 and G2 were selected such that G1 includes proteins targeting by at least three drugs in cluster 1 and at most two drugs in cluster 2, and similarly, G2, consist of proteins that are mostly targeted by drugs in cluster 2 (at least three drugs in cluster 2

and at most two drugs in cluster 1). REVIGO was also used to summarize the enriched GO terms, and the results are shown in Figure 2 and Tables S2 and S3. The cAMP signaling pathway, lipids and atherosclerosis, steroid hormone biosynthesis, and rhythmic processes and circadian rhythm are biological processes related to G1 proteins, which are mostly targeted by LY3009120, birabresib, plicamycin, and ruxolitinib. Cell cycle, cellular senescence, T-cell leukemia virus 1 infection and cell division, mitotic cell cycle, and protein phosphorylation processes are related to G2 proteins, mostly targeted by silmitasertib, ulixertinib, sapanisertib, and teniposide. Therefore, we demonstrate that the protein targets of drugs in each cluster are on different pathways and biological processes. To do homogeneity analysis of chemical structure of drugs, the dice similarity test was used to show how structurally similar the drugs are in each cluster. This measurement compares the number of chemical features shared by a pair of compounds to the average size of the total number of features present. Pairwise similarities were calculated for chemical compounds chosen from two drug clusters for inter-cluster comparison. Drugs from different clusters are less similar than drugs from the same cluster, as shown in the Figure 3A. According to the box plot, the inter-cluster similarities are less than the intra-cluster similarities in both clusters. The results of the t-test imply that the mean of inter-cluster similarities is less than the mean of intra-cluster similarities in clusters 1 and 2 (p-value < 2.2e-16 for both t-test).

Combination selection: Balancing toxicity and efficacy across clusters

As a result, we demonstrated that clusters are well-separated and that the protein targets of drugs in each cluster are involved in distinct pathways. In this novel combination strategy, we aim to select two drugs from distinct clusters while taking both toxicity and efficacy into account. The optimal combinations are those that have lower toxicity than the average toxicity and higher efficacy values than the average efficacy value for all drugs. For each

drug, the average drug response of healthy and AML patient samples in the data set are considered as toxicity and efficacy, respectively. We assume that the ideal drugs have no inhibitory effect on healthy samples but significantly influence blast cells in AML patient samples. We chose the top 5% of drugs whose toxicity is less than the average of all drug toxicity and efficacy is greater than the average of all drug efficacy. Figure 3B depicts the link between toxicity and efficacy values of 296 drugs on 81 samples. The top selected small molecule in each cluster is summarized in Table 1 and Table S4. Four chemical compounds from cluster 1 including birabresib, LY3009120, plicamycin, and ruxolitinib as well as four drugs from cluster 2 including sapanisertib, silmitasertib, teniposide, and ulixertinib were chosen for drug combination testing. According to our experimental design, the combination of drugs within a single cluster is known as negative group or intra-cluster, and the combination of drugs between clusters is considered as positive group or inter-cluster.

Enhanced efficacy and reduced toxicity in inter-cluster drug combinations on AML patient samples unveiled by cell viability drug screening

In the testing of all 16 inter-cluster and 12 intra-cluster combinations at five different concentrations, the cell viability of sixteen AML patient samples and five healthy donor samples were monitored. Patient samples with blast percentage more than 49% were chosen for testing with the Cell Titer-Glo (CTG) assay (Table S5). The average inhibition across dosages on 16 patient samples is regarded as efficacy, whereas the average inhibition across dosages on healthy samples is regarded as toxicity. The drug combinations with rectangular labels have higher efficacy and lower toxicity than the median. The proportion test (p-value = 0.006) revealed that the percentages of inter-cluster drug combinations with high efficacy (efficacy higher than the third quantile of efficacy values) and low toxicity (toxicities lower than the first quantile of toxicities) are

significantly more than random choices.

The synergy and combination ratio (CR) of drug combinations on AML and healthy samples was then calculated using synergy scoring functions has [25], bliss [26], loewe [27], and ZIP [28] (Figure 4 and S3). The same analysis was done on synergy scoring values, and it was discovered that inter-cluster drug combinations differ significantly from random choices (P-values shown in the Figure 4 A-F). The drug combinations shown with rectangular labels have the highest synergy on AML patient samples, and the lowest synergy on healthy samples. Table 2 summarizes all six plots and the significant drug combinations according to different measures are highlighted by green (inter-cluster), yellow and purple (intra-clusters). Following CTG analysis, consensus across synergy scoring functions led to the selection of the five best drug combinations out of 28 to quantify blast-specific drug responses with flow cytometry.

Cell subtype viability analysis highlights low toxicity of selected combinations

Using the CTG assay, we measure the general bone-marrow mononuclear cell (BM-MNC) sensitivity, whereas with flow cytometry analysis we measure the number of live cells among different cell populations. Following 72-hour treatment with the 5 selected combinations on 3 different samples, viability of different cell subtypes of interest was measured by flow cytometry. For each sample, there is a specific plate layout which can be found in Figure S1. We used six cell surface markers (CD14, CD15, CD45, CD38, CD117, CD34) (Table S6) to identify the major leukocyte populations present in the AML BM-MNCs: monoblasts, myelocytes, leukemic blasts, leukemic stem cells, and myeloid progenitor cells (Figure S2).

In the studied samples, the average of blasts out of CD45 positive leukocytes, was 70% in DMSO, while on average 36% $\pm$ 16% of the blasts were killed by the combinations (Table S7). Based on the results, the percentage of dead cells for all 5 combinations in

lymphocytes is considerably lower than 25% (Figure 5). More importantly selected combinations have lower synergistic effect on lymphocytes compared to the blast population, demonstrating the lower toxicity of combinations (Figure 7 and S3). The combination of JAK1/2 inhibitor (ruxolitinib) with either ERK or CSNK2A1 inhibitor has the highest efficacy and lowest toxicity which represents the important role of this target in AML. Numerous studies show the significance of the JAK/STAT signaling system in determining how hematopoietic cells react to various cytokines and growth factors [29,30]. Recently there has been increased interest in different drug combinations with ruxolitinib [31-34] and as our results show the combinations of this drug, by having the lowest toxicity, seems to be promising for AML treatment.

Blast-specific drug responses in AML: Efficacy profiles of selected combinations

We were able to assess blast-specific drug combination responses and compare them to the other combinations within different samples. Among the five tested combinations, two combinations with ruxolitinib which targets JAK1/2 were among the most efficient combinations. The combination of ruxolitinib with ulixertinib, an ERK inhibitor, exhibits the strongest efficacy against blasts, according to the results. After treatment, the combination induced 47% ± 13% cell death in blasts (Figure 5 and Table S7) with a more synergistic effect on the blast population compared to the lymphocyte population (Figure 7A). We depicted the gating of 1000 nM concentration of each drug on sample AML_3 to better understand the impact of combination therapy vs. DMSO control and single drug treated samples in Figure 6. The number of blast cells in the ruxolitinib and ulixertinib treated well was reduced to 37%, showing the largest reduction compared to all other treatments, as shown in Figure 6A. The second combination of ruxolitinib and silmitasertib, a CSNK2A1 inhibitor, showed high efficacy on blasts. On average, this combination induced death to almost half ± 14% of the blast population but had less effect

on lymphocytes (Figure 5 and Table S7). Additionally, this combination had a substantially higher inhibition rate compared to each single drug and acted synergistically towards the blast population (Figure 7A).

Given the importance of pan-RAF inhibition, we next examined LY3009120 in combination with three other drugs. The samples used for the combination of LY3009120 and sapanisertib (mTOR1/2 inhibitor), consist of 56% blast and the response for them is 40% ± 12% inhibition. To confirm that this combination is efficient, we analyzed the effect of LY3009120 and sapanisertib combination with single treated and DMSO treated cells in AML_3. In the combination treated sample, the blast cells were significantly reduced to 13% while in the individual drugs LY3009120 and sapanisertib reduced the blasts to 38% and 75%, respectively (Figure 6B). These results indicate that this combination has substantially higher inhibition rate compared to each single drug and a greater synergistic effect on blasts than on lymphocytes (Figure 7A). Ulixertinib (ERK inhibitor) is the second drug that is being used in combination with pan-RAF inhibitor. Patient samples treated with this combination, on average, contain 60% blast cells and after treatment they are reduced to 28% ± 14%. Finally, we tested the combination of LY3009120 with silmitasertib, a CSNK2A1 inhibitor on three different samples. The average blast population for these three samples is 62% and the response was 21% ± 5%. Overall, as shown in Figure 5 and 7A, all combinations have very little impact on the lymphocyte populations, demonstrating low toxicity, and significantly more impact on less differentiated malignant cells, demonstrating the efficacy of the combinations.

Increased sensitivity of AML samples to combination therapies over single drugs, regardless of genetic mutations and prognosis categories

There is a significant correlation between CTG assay and blast specific results, indicating that reduction in cell number measured by CTG, is related to the malignant cell populations

(Figure 7B and 7C). The cell viability readout for a single drug is converted to a drug sensitivity score (DSS) which is a drug sensitivity metric based on area under the dose-response curve. A greater DSS indicates higher sensitivity[35]. Strikingly, by combining selected inter-cluster drugs, the blasts were targeted, and combinations showed a synergistic effect on this population (Figure 7A). Then in order to monitor the drug responses based on genetic changes, we examined the existing mutations in selected samples that are the most significant mutations among AML patients (Figure 7A) [36,37]. To evaluate the impact of the combinations on samples bearing genetic alterations, some mutations that are frequently found in AML patients were considered (Figure 7A). *FLT3* mutation is a well-known mutant gene among AML patients and is represented in two samples. The other prevalent mutations were *NPM1, GATA2, DNMT3A, TET2, KMT2A, NRAS, SMC3* and *SRSF2*. The combinations induced a synergistic effect on the blast population, regardless of the genetic alterations. The European Leukemia Network (ELN) classifies patients into three prognosis categories: "favorable", "intermediate", or "adverse"[38]. AML patients are also classified based on morphological features which is named French-American-British Classification (FAB) [39]. Regardless of sample type, we observed a synergistic effect following treatment. Importantly, after therapy, we noticed a synergistic effect in all samples, indicating that these combinations are effective at combating the heterogeneity of the AML disease. It has been demonstrated that drugs should target the less differentiated leukemic blasts to achieve the best response in patients [6]. Given these two facts—the presence of the most relevant mutations and the prevalence of blast cells in the samples— the combinations seem to be promising for treatment.

Efficacy and toxicity of the novel combinations compared to first-line treatment in AML

In the following analysis, we compared the proposed combinations in this study (ruxolitinib-ulixertinib and LY3009120-sapanisertib) with two FDA-approved combinations (venetoclax-

azacitidine and venetoclax-cytarabine), as well as the investigational combination of venetoclax-ruxolitinib. As illustrated in Figure 8, venetoclax-ruxolitinib demonstrates the highest efficacy on both blast cells and lymphocytes compared to the other combinations. This dual efficacy profile is a noteworthy advantage; however, it comes at the cost of heightened toxicity, as indicated by our results.

Conversely, the novel combinations, ruxolitinib-ulixertinib and LY3009120-sapanisertib, show comparable efficacy in targeting blast populations as the established combinations. Notably, there is no significant difference in terms of efficacy (p-values are shown in Figure 8). However, these two combinations have a significant advantage in demonstrating lower toxicity compared to first-line combinations, particularly for lymphocytes. The effect of ruxolitinib-ulixertinib and LY3009120-sapanisertib on blast lymphocyte population is significantly lower than all other combinations except for venetoclax-cytarabine (p-value = 0.25) which is not significant but still is lower. This reduction in toxicity suggests these combinations can offer effective treatment while minimizing side effects associated with prevalence therapies.

Discussion

In this study we employed a nominal data mining approach to construct a weighted bipartite network for the selection of the most effective [10], as well as the least toxic drugs. The selected combinations inhibit important signaling pathways and included pan-RAF inhibitors, JAK1/2 inhibitors, BET family inhibitors, topoisomerase II inhibitor, CSNK2A1 inhibitors, ERK inhibitors, mTOR1/2 inhibitors, and DNA binding drugs.

The MAPK (RAS/RAF/MEK/ERK) signaling pathway is hyperactivated in AML patients, leading to leukemogenesis, leukemia progression, and chemo resistance [40-43]. Since, targeting RAS and ERK remains challenging, pan-RAF inhibitors are an interesting new pharmacological class in this context [44,45]. Recent studies demonstrated that the pan-RAF inhibitor LY3009120 induces growth inhibition and apoptosis in RAS-mutated AML cell lines [46,47]. Another component of the MAPK pathway is ERK, and the ERK inhibitor ulixertinib is a promising early efficacy agent for treating patients with tumors harboring alterations in the MAPK pathway [48]. The ERK pathway is activated in approximately 30% of all human cancers via *RAS, BRAF,* or *MAP2K1 (MEK1)* activating mutations and thus targeted therapeutics are vital to treating ERK pathway–activated human cancers [49]. Bhagwat et al. demonstrated the efficacy of LY3214996 as an ERK inhibitor to delay or reverse resistance to BRAF and MEK inhibitor therapy. They also demonstrated a synergistic effect of the combination of LY3214996 with a pan-RAF inhibitor, LY3001920, in a KRAS-mutant colorectal cancer xenograft model [50]. Moreover, here we identified ulixertinib and LY3009120 as an inter-cluster combination with high efficacy and low toxicity. Upon further analysis, we found two combinations of ulixertinib and three combinations of LY3009120 among the five most efficient and synergistic combinations.

The other signaling pathway is JAK signaling, which plays critical roles in several important intracellular signaling pathways [51,52]. In a number of leukemias, aberrations of the JAK/STAT

pathway and constitutive STAT activation have been well described [53]. Ruxolitinib has been approved as a non-selective JAK1/2 inhibitor for patients with intermediate to high risk primary or secondary myelofibrosis [54]. Ruxolitinib, by inhibiting JAK 1/2, reduce activation of JAK-signal transducers and lower down the transcription (STAT) signaling [55]. Based on our computational analysis, CTG results, and flow cytometry analysis, we revealed that combinations of ruxolitinib with ulixertinib and silmitasertib are the most blast-specific compounds, while having minor effect on lymphocytes in AML *ex vivo* screening.

Next, we examined the effect of Bromodomain and Extra-Terminal motif (BET) protein inhibitors on cancer cells as BET proteins are often altered in cancer. While bromodomain inhibition is effective, not all patients benefit from it and become resistant over time [56]. Researchers recently reported the efficacy of combined JAK/BET inhibition on cytokine production, BM fibrosis, and tumor burden *in vivo* [57], leading to complete reversal of reticulin fibrosis in mice. In our model, this drug was classified among effective drugs in cluster 1 and based on the CTG assay, in combination with sapanisertib, ulixertinib, and teniposide can be potential compound for the treatment of AML patients.

The other drug that was selected is teniposide which is a chemotherapy medicine used to treat solid tumors and leukemia, typically in combination with other antineoplastic agents. This agent causes DNA damage in proliferating cells by inhibiting topoisomerase II. Recently, it has been proven that teniposide not only inhibits topoisomerase II but also inhibits MYB, transcription factor, activity and expression [58]. Topoisomerase II inhibitors' ever-evolving role in the treatment of AML has led to an increase in their utilization in combination therapies [59]. Here in this study, we identified the combination of teniposide and birabresib among the most effective compounds with low toxicity.

The next drug is silmitasertib that inhibits CSNK2A1. Studies showed increased expression of this kinase in AML cells, which contributes to several biological processes

related to cancer progression such as apoptosis, cell growth, proliferation and transcription [60]. Silmitasertib is currently being evaluated in clinical trials for the treatment of multiple malignancies [61]. Hereby, considering the importance of pan-RAF and CSNK2A1 inhibitors, targeting these two pathways simultaneously might be a promising treatment. Additionally, as we suggested, the combination of silmitasertib and ruxolitinib could be considered as potential combinations for treating AML patients.

We then, studied the effect of plicamycin, which inhibits RNA synthesis by binding to GC-rich regions of DNA. Plicamycin has potent anti-tumor effects, both as mono-therapy and in combination with anti-tumor drugs [62]. A highly selective adenosine triphosphate-competitive inhibitor of mTOR kinase, named sapanisertib has been also included in this study. Sapanisertib has demonstrated antitumor activity in AML by inhibiting both mTORC1 and mTORC2 [63]. Sapanisertib in combination with LY3009120, birabresib or ulixertinib has synergistic effect in AML samples (Figure 4).

Lastly, we thoroughly compared the two FDA-approved combinations (venetoclax-azacitidine and venetoclax-cytarabine) and one investigational combination (venetoclax-ruxolitinib) with the novel combinations suggested in this study, namely ruxolitinib-ulixertinib and LY3009120-sapanisertib. Notably, the outcomes validated the comparability of the suggested combinations' efficacy with first-line combinations in this investigation. There is no significant difference in efficacy on blast cells, between proposed combinations and first-line AML combinations. Significantly, the toxicity of selected combinations is lower than others, except for venetoclax-cytarabine, which indicates that proposed combinations might offer both effective treatment and a reduced side effect compared to standard AML combinations.

In summary, we proposed effective drug combinations for AML patients with the highest efficacy and lowest toxicity based on nominal data mining method and *ex vivo* drug

sensitivity assay. The combinations were tested on three different samples, and the results indicate that the combinations of ruxolitinib-ulixertinib and sapanisertib-LY3009120 have the highest synergistic effect, the highest efficacy on blasts, and the lowest toxicity. Although the approach of combining targeted agents suffers from cumulative toxicity effects [64], we have demonstrated that our approach overcomes this limitation in designing a drug combination in AML. Considering the importance of toxicity, in all steps we considered toxicity as an important factor for the selection of combinations with the lowest effect on healthy cells. Standard chemotherapy kills most of the blasts as well as other cell types and has a high value of toxicity [6], while recommended combinations in this study are effective on blasts, but have lower toxicity on other cell populations.

Acknowledgments

We thank the patients and donors who participated in the study. Drug screening was carried out at the FIMM High Throughput Biomedicine Unit (HTB), which is hosted by the University of Helsinki and supported by HiLIFE and Biocenter Finland. Alun Parsons is gratefully acknowledged for his technical support. We also appreciate comments from Marc Baumann, Julio Saez-Rodriguez and Farnaz Barneh. This study was financially supported by the Research Council in Finland [grant 332454 to M.J.; grants 320185, 334781, 357686 to C.A.H.], and Jane & Aatos Erkko Foundation [grant 220031 to M.J.], and the Sigrid Jusélius Foundation [grant to C.A.H.].

Authorship Contributions

M.J. conceived of the study and designed research questions. M.J. and C.A.H. oversaw the scientific direction, supervised the project, and assisted with the manuscript. Also C.A.H. contributed resources including patient samples. M.M. led the computational and statistical analysis, interpreted the data, and assisted with study design, while E.G., T.R., and J.S. designed and developed the experimental methods for cell viability analysis. J.M. and F.I. contributed to the interpretation of the findings for drug sensitivity analysis. M.M and S.M contributed bone marrow samples from healthy donors.

† M.M. contributed equally to this work with E.G.

Conflict of Interest

C.A.H. has received research funding from BMS/Celgene, Kronos Bio, Novartis, Oncopeptides, Orion Pharma, WNTResearch, Glykos Finland, and IMI2 projects HARMONY and HARMONYPLUS, plus personal fees from Amgen and Autolus unrelated to this work. The remaining authors declare no competing interests.

Data availability statement

The data that support the findings of this study and all code for data analysis are openly available at https://github.com/jafarilab/DrugComb_AML.

References

1 Bowman, R. L., Busque, L. & Levine, R. L. Clonal hematopoiesis and evolution to hematopoietic malignancies. *Cell stem cell* **22**, 157--170 (2018).

2 Grzywa, T. M., Paskal, W. & Wodarski, P. K. Intratumor and intertumor heterogeneity in melanoma. *Translational oncology* **10**, 956--975 (2017).

3 Bennett, J. M. *et al.* Proposals for the classification of the acute leukaemias French-American-British (FAB) co-operative group. *British journal of haematology* **33**, 451--458 (1976).

4 Peipert, J. D. *et al.* Patient-reported outcomes predict overall survival in older patients with acute myeloid leukemia. *Journal of Geriatric Oncology* **13**, 935--939 (2022).

5 Daver, N. *et al.* New directions for emerging therapies in acute myeloid leukemia: The next chapter. *Blood cancer journal* **10**, 1--12 (2020).

6 Kuusanmki, H. & Lepp. Phenotype-based drug screening reveals association between venetoclax response and differentiation stage in acute myeloid leukemia. *Haematologica* **105**, 708 (2020).

7 Intlekofer, A. M. *et al.* Acquired resistance to IDH inhibition through trans or cis dimer-interface mutations. *Nature* **559**, 125--129 (2018).

8 Lopez, J. S. & Banerji, U. Combine and conquer: challenges for targeted therapy combinations in early phase trials. *Nature reviews Clinical oncology* **14**, 57--66 (2017).

9 Ianevski, A. *et al.* Patient-tailored design for selective co-inhibition of leukemic cell subpopulations. *Science advances* **7**, eabe4038 (2021).

10 Jafari, M. *et al.* Bipartite network models to design combination therapies in acute myeloid leukaemia. *Nature communications* **13**, 1--12 (2022).

11 Malani, D. *et al.* Implementing a Functional Precision Medicine Tumor Board for Acute Myeloid LeukemiaAML Functional Molecular Precision Medicine. *Cancer Discovery* **12**, 388--401 (2022).

12 Ianevski, A., Timonen, S., Kononov, A., Aittokallio, T. & Giri, A. K. SynToxProfiler: An interactive analysis of drug combination synergy, toxicity and efficacy. *PLoS computational biology* **16**, e1007604 (2020).

13 Sarma, A. *et al.* Expression of aberrant CD markers in acute leukemia: A study of 100 cases with immunophenotyping by multiparameter flowcytometry. *Cancer Biomarkers* **15**, 501--505 (2015).

14 Blondel, V. D., Guillaume, J.-L., Lambiotte, R. & Lefebvre, E. Fast unfolding of communities in large networks. *Journal of statistical mechanics: theory and experiment* **2008**, P10008 (2008).

15 Tang, J. *et al.* Drug target commons: a community effort to build a consensus knowledge base for drug-target interactions. *Cell chemical biology* **25**, 224--229 (2018).

16 Park, J. *et al.* Pan-RAF inhibitor LY3009120 is highly synergistic with low-dose cytarabine, but not azacitidine, in acute myeloid leukemia with RAS mutations. *Oncology letters* **22**, 1-11 (2021).

17 Klein, K., Stoiber, D., Sexl, V. & Witalisz-Siepracka, A. Untwining anti-tumor and immunosuppressive effects of JAK inhibitors—a strategy for hematological malignancies? *Cancers* **13**, 2611 (2021).

18 Gilan, O. *et al.* Selective targeting of BD1 and BD2 of the BET proteins in cancer and immunoinflammation. *Science* **368**, 387-394 (2020).

19 Albertini, V. *et al.* Novel GC-rich DNA-binding compound produced by a genetically engineered mutant of the mithramycin producer Streptomyces argillaceus exhibits improved transcriptional repressor activity: implications for cancer therapy. *Nucleic acids research* **34**, 1721-1734 (2006).

20 Blanco-Aparicio, C. & Carnero, A. Pim kinases in cancer: diagnostic, prognostic and treatment opportunities. *Biochemical pharmacology* **85**, 629-643 (2013).

21 Hayes, T. K. & Der, C. J. Targeting the Raf-MEK-ERK mitogen-activated protein kinase cascade for the treatment of RAS mutant cancers. *Ras Superfamily Small G Proteins: Biology and Mechanisms 1: General Features, Signaling*, 135-156 (2014).
22 Shimizu, T. *et al*. A phase 1 study of Sapanisertib (TAK-228) in East Asian patients with advanced nonhematological malignancies. *Targeted oncology*, 1-10 (2022).
23 Economides, M. P., McCue, D., Borthakur, G. & Pemmaraju, N. Topoisomerase II inhibitors in AML: past, present, and future. *Expert opinion on pharmacotherapy* **20**, 1637-1644 (2019).
24 Ge, S. X., Jung, D. & Yao, R. ShinyGO: a graphical gene-set enrichment tool for animals and plants. *Bioinformatics* **36**, 2628--2629 (2020).
25 Berenbaum, M. C. What is synergy? *Pharmacological reviews* **41**, 93--141 (1989).
26 Bliss, C. I. The toxicity of poisons applied jointly 1. *Annals of applied biology* **26**, 585--615 (1939).
27 Loewe, S. The problem of synergism and antagonism of combined drugs. *Arzneimittelforschung* **3**, 285--290 (1953).
28 Yadav, B., Wennerberg, K., Aittokallio, T. & Tang, J. Searching for drug synergy in complex dose--response landscapes using an interaction potency model. *Computational and structural biotechnology journal* **13**, 504--513 (2015).
29 Ferrajoli, A., Faderl, S., Ravandi, F. & Estrov, Z. The JAK-STAT pathway: a therapeutic target in hematological malignancies. *Current cancer drug targets* **6**, 671--679 (2006).
30 Eghtedar, A. *et al*. Phase 2 study of the JAK kinase inhibitor ruxolitinib in patients with refractory leukemias, including postmyeloproliferative neoplasm acute myeloid leukemia. *Blood, The Journal of the American Society of Hematology* **119**, 4614--4618 (2012).
31 Borate, U. *et al*. Novel Combination Therapy of Venetoclax and Ruxolitinib in the Treatment of Patients with Relapsed/Refractory Acute Myeloid Leukemia. *Blood* **138**, 2333 (2021).
32 Verbeke, D. *et al*. Ruxolitinib synergizes with dexamethasone for the treatment of T-cell acute lymphoblastic leukemia. *Hemasphere* **3** (2019).
33 Dal Bello, R. *et al*. A multiparametric niche-like drug screening platform in acute myeloid leukemia. *Blood Cancer Journal* **12**, 1--12 (2022).
34 Karjalainen, R. *et al*. JAK1/2 and BCL2 inhibitors synergize to counteract bone marrow stromal cell--induced protection of AML. *Blood, The Journal of the American Society of Hematology* **130**, 789--802 (2017).
35 Yadav, B. *et al*. (2014).
36 Papaemmanuil, E. *et al*. Genomic classification and prognosis in acute myeloid leukemia. *New England Journal of Medicine* **374**, 2209--2221 (2016).
37 Tyner, J. W. *et al*. Functional genomic landscape of acute myeloid leukaemia. *Nature* **562**, 526--531 (2018).
38 Rausch, C. *et al*. Validation of the 2022 European Leukemianet genetic risk stratification of acute myeloid leukemia. *Blood* **140**, 3408--3409 (2022).
39 Hasserjian, R. P. Controversies in the recent (2016) World Health Organization classification of acute myeloid leukemia. *Best Practice & Research Clinical Haematology* **34**, 101249 (2021).
40 Ricciardi, M. R. *et al*. Quantitative single cell determination of ERK phosphorylation and regulation in relapsed and refractory primary acute myeloid leukemia Tandem-duplicated Flt3 constitutively activates STAT5 and MAP kinase and introduces autonomous cell growth in IL-3-dependent cell lines. *Leukemia* **19**, 1543--1549 (2005).
41 Steelman, L. S. *et al*. Roles of the Ras/Raf/MEK/ERK pathway in leukemia therapy. *Leukemia* **25**, 1080--1094 (2011).
42 Chang, F. *et al*. Signal transduction mediated by the Ras/Raf/MEK/ERK pathway from cytokine receptors to transcription factors: potential targeting for therapeutic intervention. *Leukemia (08876924)* **17** (2003).

43 Kornblau, S. M. *et al*. Simultaneous activation of multiple signal transduction pathways confers poor prognosis in acute myelogenous leukemia. *Blood* **108**, 2358--2365 (2006).
44 Cox, A. D., Fesik, S. W., Kimmelman, A. C., Luo, J. & Der, C. J. Drugging the undruggable RAS: Mission possible? *Nature reviews Drug discovery* **13**, 828--851 (2014).
45 Tambe, M. *et al*. Pan-RAF inhibition induces apoptosis in acute myeloid leukemia cells and synergizes with BCL2 inhibition. *Leukemia* **34**, 3186--3196 (2020).
46 Khoury, J. D. *et al*. Pan-RAF inhibition shows anti-leukemic activity in RAS-mutant acute myeloid leukemia cells and potentiates the effect of sorafenib in cells with FLT3 mutation. *Cancers* **12**, 3511 (2020).
47 Park, J. *et al*. Pan-RAF inhibitor LY3009120 is highly synergistic with low-dose cytarabine, but not azacitidine, in acute myeloid leukemia with RAS mutations. *Oncology letters* **22**, 1--11 (2021).
48 idecabtagene Vicleucel, C. A. R. T. C. T. FDA updates highlighting the Latest Cancer Treatments. *Oncology Times* (2020).
49 Roberts, P. J. & Der, C. J. Targeting the Raf-MEK-ERK mitogen-activated protein kinase cascade for the treatment of cancer. *Oncogene* **26**, 3291--3310 (2007).
50 Bhagwat, S. V. *et al*. ERK inhibitor LY3214996 targets ERK pathway--driven cancers: a therapeutic approach toward precision medicine. *Molecular cancer therapeutics* **19**, 325--336 (2020).
51 Ihle, J. N. & Kerr, I. M. Jaks and Stats in signaling by the cytokine receptor superfamily. *Trends in Genetics* **11**, 69--74 (1995).
52 Rawlings, J. S., Rosler, K. M. & Harrison, D. A. The JAK/STAT signaling pathway. *Journal of cell science* **117**, 1281--1283 (2004).
53 Lin, T. S., Mahajan, S. & Frank, D. A. STAT signaling in the pathogenesis and treatment of leukemias. *Oncogene* **19**, 2496--2504 (2000).
54 Furqan, M., Mukhi, N., Lee, B. & Liu, D. Dysregulation of JAK-STAT pathway in hematological malignancies and JAK inhibitors for clinical application. *Biomarker research* **1**, 1--10 (2013).
55 McKeage, K. Ruxolitinib: a review in polycythaemia vera. *Drugs* **75**, 1773--1781 (2015).
56 Bechter, O. & Schffski, P. Make your best BET: The emerging role of BET inhibitor treatment in malignant tumors. *Pharmacology & Therapeutics* **208**, 107479 (2020).
57 Kleppe, M. *et al*. Dual targeting of oncogenic activation and inflammatory signaling increases therapeutic efficacy in myeloproliferative neoplasms. *Cancer cell* **33**, 29--43 (2018).
58 Yusenko, M., Jakobs, A. & Klempnauer, K.-H. A novel cell-based screening assay for small-molecule MYB inhibitors identifies podophyllotoxins teniposide and etoposide as inhibitors of MYB activity. *Scientific reports* **8**, 1--11 (2018).
59 Economides, M. P., McCue, D., Borthakur, G. & Pemmaraju, N. Topoisomerase II inhibitors in AML: past, present, and future. *Expert opinion on pharmacotherapy* **20**, 1637--1644 (2019).
60 Kang, K.-W. *et al*. A Proteomic Approach to Understand the Clinical Significance of Acute Myeloid Leukemia--Derived Extracellular Vesicles Reflecting Essential Characteristics of Leukemia. *Molecular & Cellular Proteomics* **20** (2021).
61 Roffey, S. E. & Litchfield, D. W. CK2 Regulation: Perspectives in 2021. *Biomedicines* **9**, 1361 (2021).
62 Chen, C. & Lan, M. S. A promoter-driven assay for INSM1-associated signaling pathway in neuroblastoma. *Cellular Signalling* **76**, 109785 (2020).
63 Shimizu, T. *et al*. A Phase 1 Study of Sapanisertib (TAK-228) in East Asian Patients with Advanced Nonhematological Malignancies. *Targeted oncology* **17**, 15--24 (2022).
64 Tannock, I. F. & Hickman, J. A. Molecular screening to select therapy for advanced cancer? *Annals of Oncology* **30**, 661-663 (2019).

Figure legends

Fig. 1. Schematic outline of the study. Data pre-processing began after data collection, which was followed by full matrix extraction, weighted bipartite network reconstruction, and computational validation. After the selection of the best combinations, bone marrow and peripheral blood samples from both healthy individuals (n=5) and AML patients (n= 16) were subjected to drug sensitivity assessment. For ATP-based viability assay the study design contains 8 drugs and 28 combinations in 384-well plates, each drug with 5 different concentrations and two replicate. The single cell sensitivity assay using the iQue® Screener PLUS flow cytometer was performed in 384-well plates to monitor drug effects on cell sub-types. The study design contains 5 drugs and 3 combinations, all with two replicates and five concentrations. For sapanisertib, the drug concentrations are 0.1, 1, 10, 100, and 1000 nM, and for all other drugs are 1, 10, 100, 1000, and 10000 nM.

Fig. 2. Sankey plot of enriched (A) KEGG signalling pathways and (B) GO biological processes related to target protein clusters PPT1 and PPT2. Each rectangle on the right side represents a pathway or biological process, and the size of each rectangle illustrates the degree of connectivity of each pathway. Each biological process or pathway is represented by a unique color. GO and KEGG pathway enrichment analysis on proteins that are merely targets by drugs in one cluster. G1 (G2) includes proteins that are targeted by at least three drugs in cluster1 (cluster2) (155 and 141 drugs). (C) Biological processes (BPs) of G1, (D) Biological processes (BPs) of G2, (E) KEGG pathway related to G1 proteins and (F) KEGG pathway related to G2 proteins. The size of the node corresponds to number of genes, the x-axis is Fold Enrichment and the color of bars indicates the negative logarithm of Fold Enrichment.

Fig. 3. Comparative analysis of dice similarity and drug efficacy-toxicity profiles in AML therapy. (A) Box plot of dice similarity coefficient indices comparing intra-cluster 1 and 2 to inter-cluster compound pairs. P-value is generated using Wilcoxon signed-rank test, shown in red color. (B) The toxicity and efficacy of 296 drugs. Inset plot shows the relationship between toxicity and efficacy. Top five percent of drugs whose toxicity is less than the average of all drug toxicity and whose efficacy is greater than the average of all drug efficacy are in blue, and their name is shown in rectangle labels.

Fig. 4. Drug combinations' synergy scores on 16 AML samples and 5 healthy samples. X-axis depicts the synergy on AML samples and the Y-axis represents the synergy on healthy samples. The median inhibition on AML and healthy samples, respectively, is shown by the dashed lines in red and blue. There are three groupings: clusters 1, 2, and inter-cluster, and the color of each dot indicates each of these groups.

Fig. 5. The cell viability assay (CTG) and response of different cell populations to 5 selected combinations using flow cytometry assay. Response signifies the percentage of dead cells following a 72-hour treatment. For each combination three different samples, distinguished by the color of points, were treated with three doses (10, 100, 1000), which are illustrated by different shapes of points. The colors in each cell group facet corresponds to a specific drug combination.

Fig. 6. Flow cytometry scatter plots showing the effects of drug combinations on cell populations, along with comparisons to DMSO and single drug treated samples. (A) This figure illustrates the effects of ruxolitinib and ulixertinib combination and (B) LY3009120 and sapanisertib combination on blasts, monocytic cells (CD14+) and lymphocytes after 72h drug treatment. Numbers are presenting the percentage of cell counts in each cell population. The plot represents concentration of 1000 nM on sample AML_3.

Fig. 7. Characteristics of drug responses and correlation analysis in AML treatment: Comprehensive flow cytometry and CTG assessment. (A)Heat map showing characteristics of single agent and combinations response measured by flow cytometry readout. Blast-specific response of single drugs is highlighted according to drug sensitivity score (DSS) values with dark blue corresponding to high DSS value and white to low DSS value. Blast-specific and lymphocyte-specific response combinations in 1000 nM are highlighted according to percentage of apoptotic/dead cells, with dark blue in blast and red for lymphocyte corresponding to high percentage and white to a low percentage of apoptotic/dead cells. The synergistic effect of the drug combination was assessed based on the HSA synergistic score in 1000 nM on blast cells shown in blue and lymphocytes shown in red. (B) The correlation between responses measured by CTG and flow cytometry on five single drugs ruxolitinib, silmitasertib, ulixertinib, LY3009120, and sapanisertib, and (C) five drug combinations sapanisertib-LY3009120, ulixertinib-ruxolitinib, silmitasertib-ruxolitinib, silmitasertib-LY3009120, and ulixertinib-LY300912.

Fig. 8. Flow cytometry assay of selected combinations compared to first-line AML combinations. Response signifies the percentage of dead cells following 72-hour treatment. Each combination has been tested on different samples at 50 nM concentration for venetoclax and 1000 nM for the other drugs. Red asterisks define the average response for each combination and colored dots represent different samples. Each panel also represents six p-values resulting from the Wilcoxon signed-rank tests to compare statistically two proposed combinations with three other combinations (including two first-line treatments and one investigational combination) for AML.

Table legends

Table 1. The selected chemical compounds from two clusters of drugs in the drug similarity network.

Table 1. Selected drug combinations sorted by synergy scoring functions. Highlighted in green (inter-cluster), yellow (intra-cluster 1), and purple (intra-cluster 2). Inh stands for the average of inhibition of drug combinations on dosages, ZIP, hsa, bliss, and loewe are synergy scorings and CR is the combination ratio.

Figure 1

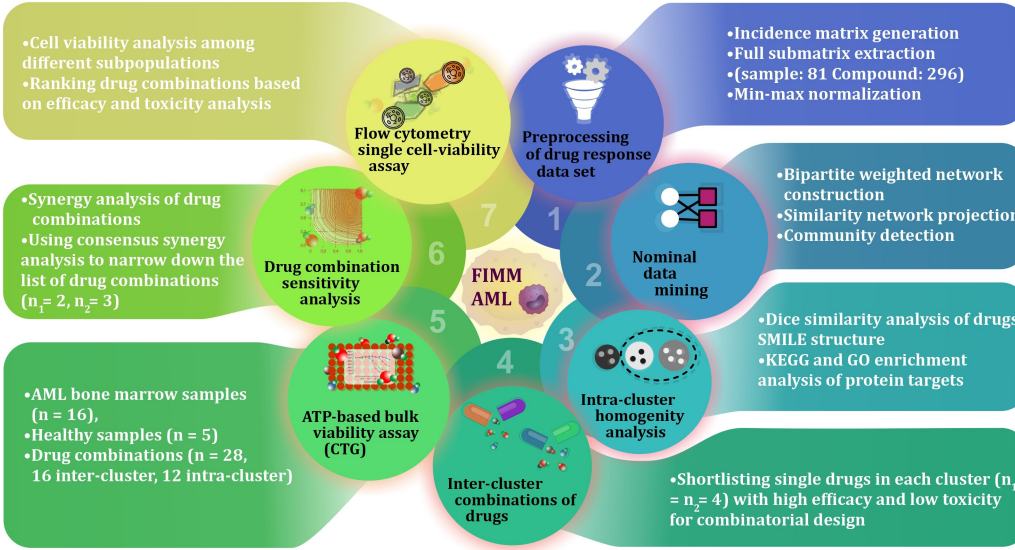
•Cell viability analysis among different subpopulations
•Ranking drug combinations based on efficacy and toxicity analysis
Flow cytometry single cell-viability assay
Preprocessing of drug response data set
•Incidence matrix generation
•Full submatrix extraction
•(sample: 81 Compound: 296)
•Min-max normalization
•Synergy analysis of drug combinations
•Using consensus synergy analysis to narrow down the list of drug combinations (n_1= 2, n_2= 3)
Drug combination sensitivity analysis
7
1
6
FIMM AML
2
Nominal data mining
•Bipartite weighted network construction
•Similarity network projection
•Community detection
5
3
4
•Dice similarity analysis of drugs SMILE structure
•KEGG and GO enrichment analysis of protein targets
•AML bone marrow samples (n = 16),
•Healthy samples (n = 5)
•Drug combinations (n = 28, 16 inter-cluster, 12 intra-cluster)
ATP-based bulk viability assay (CTG)
Intra-cluster homogenity analysis
Inter-cluster combinations of drugs
•Shortlisting single drugs in each cluster (n_1 = n_2= 4) with high efficacy and low toxicity for combinatorial design

Figure 2

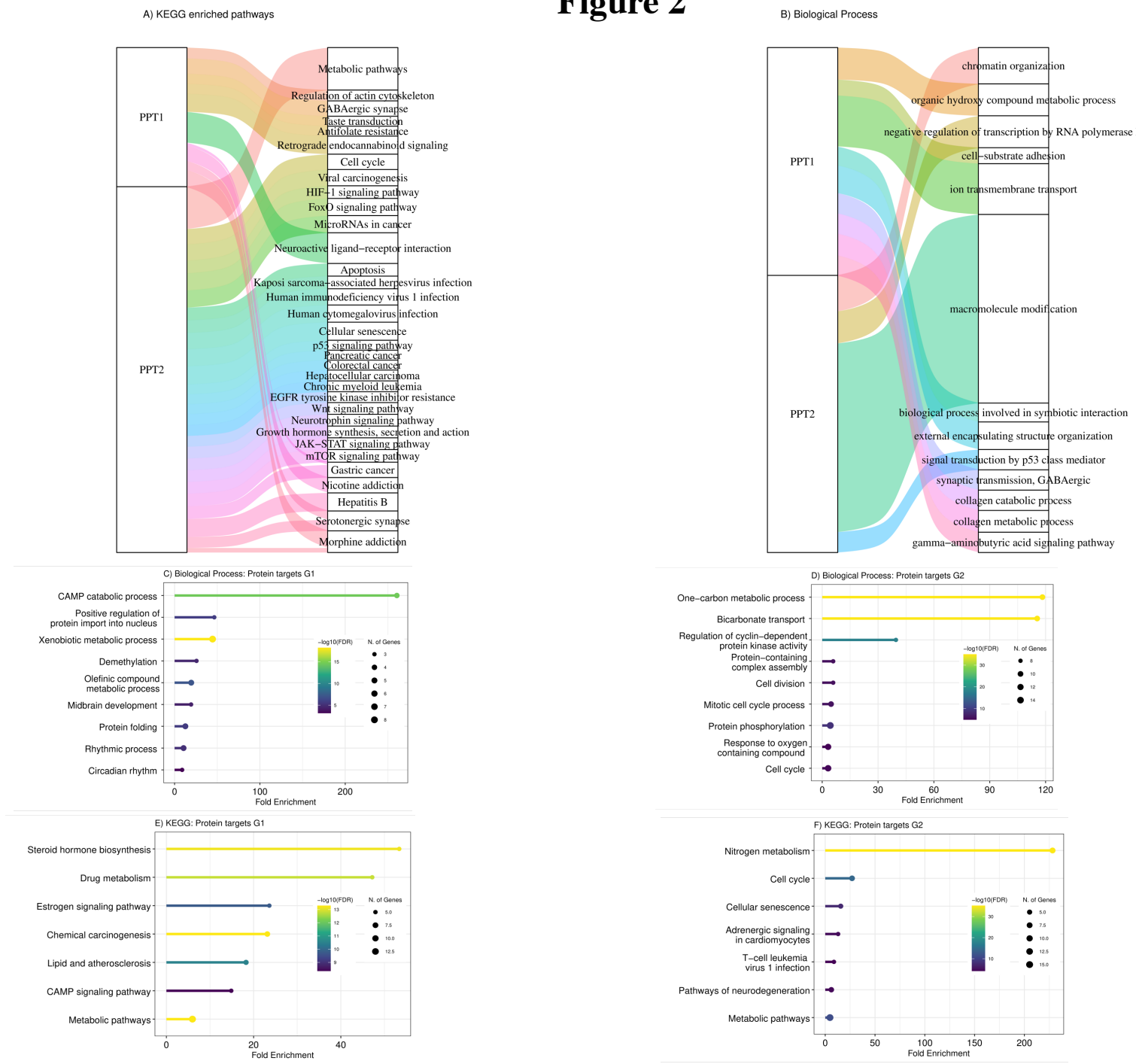
A) KEGG enriched pathways
PPT1
PPT2
Metabolic pathways
Regulation of actin cytoskeleton
GABAergic synapse
Taste transduction
Antifolate resistance
Retrograde endocannabinoid signaling
Cell cycle
Viral carcinogenesis
HIF−1 signaling pathway
FoxO signaling pathway
MicroRNAs in cancer
Neuroactive ligand−receptor interaction
Apoptosis
Kaposi sarcoma−associated herpesvirus infection
Human immunodeficiency virus 1 infection
Human cytomegalovirus infection
Cellular senescence
p53 signaling pathway
Pancreatic cancer
Colorectal cancer
Hepatocellular carcinoma
Chronic myeloid leukemia
EGFR tyrosine kinase inhibitor resistance
Wnt signaling pathway
Neurotrophin signaling pathway
Growth hormone synthesis, secretion and action
JAK−STAT signaling pathway
mTOR signaling pathway
Gastric cancer
Nicotine addiction
Hepatitis B
Serotonergic synapse
Morphine addiction
B) Biological Process
PPT1
PPT2
chromatin organization
organic hydroxy compound metabolic process
negative regulation of transcription by RNA polymerase
cell−substrate adhesion
ion transmembrane transport
macromolecule modification
biological process involved in symbiotic interaction
external encapsulating structure organization
signal transduction by p53 class mediator
synaptic transmission, GABAergic
collagen catabolic process
collagen metabolic process
gamma−aminobutyric acid signaling pathway
C) Biological Process: Protein targets G1
CAMP catabolic process
Positive regulation of protein import into nucleus
Xenobiotic metabolic process
Demethylation
Olefinic compound metabolic process
Midbrain development
Protein folding
Rhythmic process
Circadian rhythm
−log10(FDR)
N. of Genes
Fold Enrichment
D) Biological Process: Protein targets G2
One−carbon metabolic process
Bicarbonate transport
Regulation of cyclin−dependent protein kinase activity
Protein−containing complex assembly
Cell division
Mitotic cell cycle process
Protein phosphorylation
Response to oxygen containing compound
Cell cycle
−log10(FDR)
N. of Genes
Fold Enrichment
E) KEGG: Protein targets G1
Steroid hormone biosynthesis
Drug metabolism
Estrogen signaling pathway
Chemical carcinogenesis
Lipid and atherosclerosis
CAMP signaling pathway
Metabolic pathways
−log10(FDR)
N. of Genes
Fold Enrichment
F) KEGG: Protein targets G2
Nitrogen metabolism
Cell cycle
Cellular senescence
Adrenergic signaling in cardiomyocytes
T−cell leukemia virus 1 infection
Pathways of neurodegeneration
Metabolic pathways
−log10(FDR)
N. of Genes
Fold Enrichment

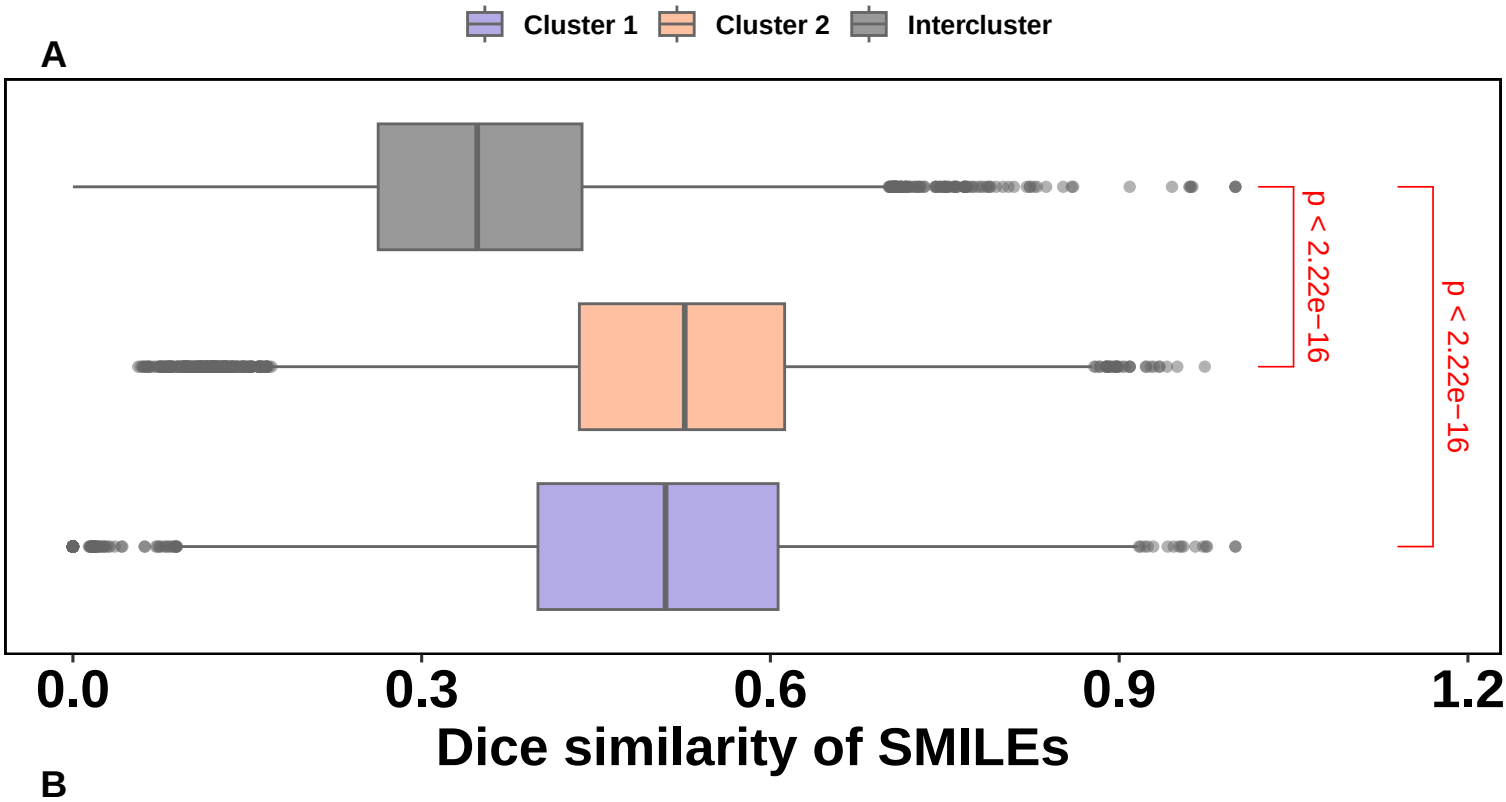
A
Cluster 1
Cluster 2
Intercluster
p < 2.22e−16
p < 2.22e−16
0.0
0.3
0.6
0.9
1.2
Dice similarity of SMILEs

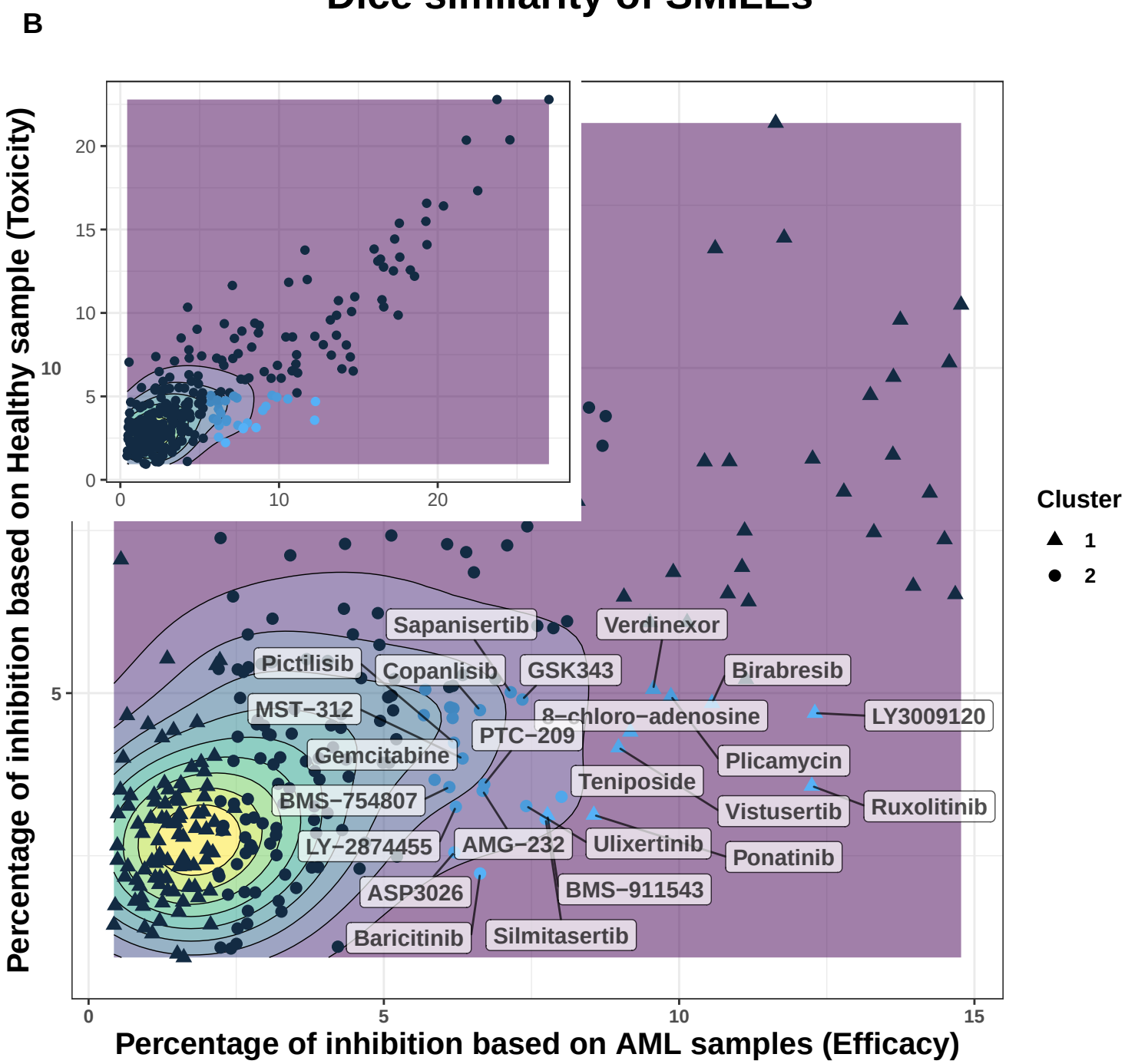
B
Percentage of inhibition based on Healthy sample (Toxicity)
Percentage of inhibition based on AML samples (Efficacy)
Cluster
1
2
Sapanisertib
Verdinexor
Pictilisib
Copanlisib
GSK343
Birabresib
MST−312
8−chloro−adenosine
LY3009120
PTC−209
Gemcitabine
Plicamycin
Teniposide
BMS−754807
Vistusertib
Ruxolitinib
LY−2874455
AMG−232
Ulixertinib
Ponatinib
ASP3026
BMS−911543
Baricitinib
Silmitasertib

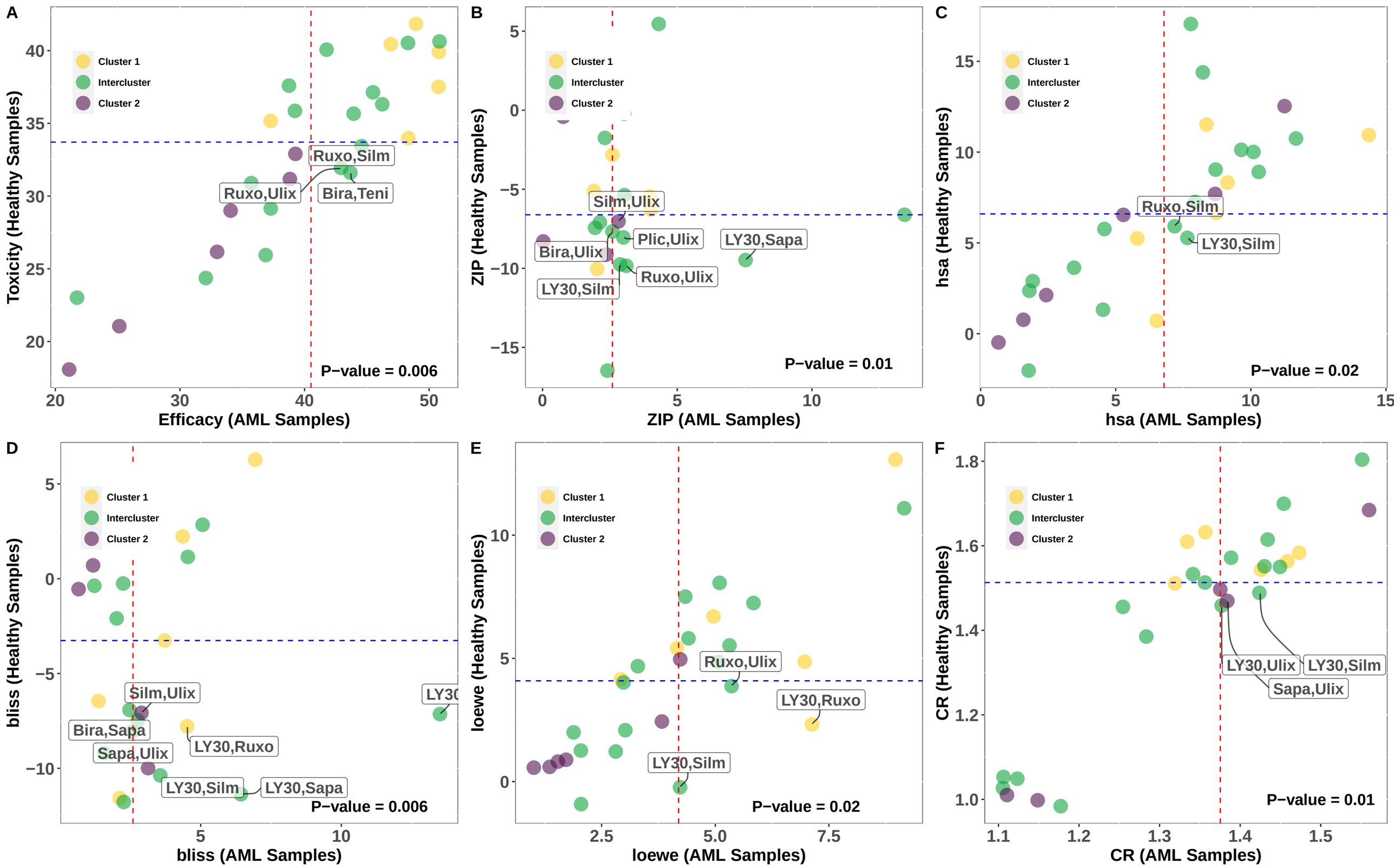
A
Cluster 1
Intercluster
Cluster 2
Ruxo,Silm
Ruxo,Ulix
Bira,Teni
P−value = 0.006
Toxicity (Healthy Samples)
Efficacy (AML Samples)
B
Silm,Ulix
Plic,Ulix
LY30,Sapa
Bira,Ulix
Ruxo,Ulix
LY30,Silm
P−value = 0.01
ZIP (Healthy Samples)
ZIP (AML Samples)
C
Ruxo,Silm
LY30,Silm
P−value = 0.02
hsa (Healthy Samples)
hsa (AML Samples)
D
Silm,Ulix
Bira,Sapa
Sapa,Ulix
LY30,Ruxo
LY30,Silm
LY30,Sapa
P−value = 0.006
bliss (Healthy Samples)
bliss (AML Samples)
E
Ruxo,Ulix
LY30,Ruxo
LY30,Silm
P−value = 0.02
loewe (Healthy Samples)
loewe (AML Samples)
F
LY30,Ulix
LY30,Silm
Sapa,Ulix
P−value = 0.01
CR (Healthy Samples)
CR (AML Samples)

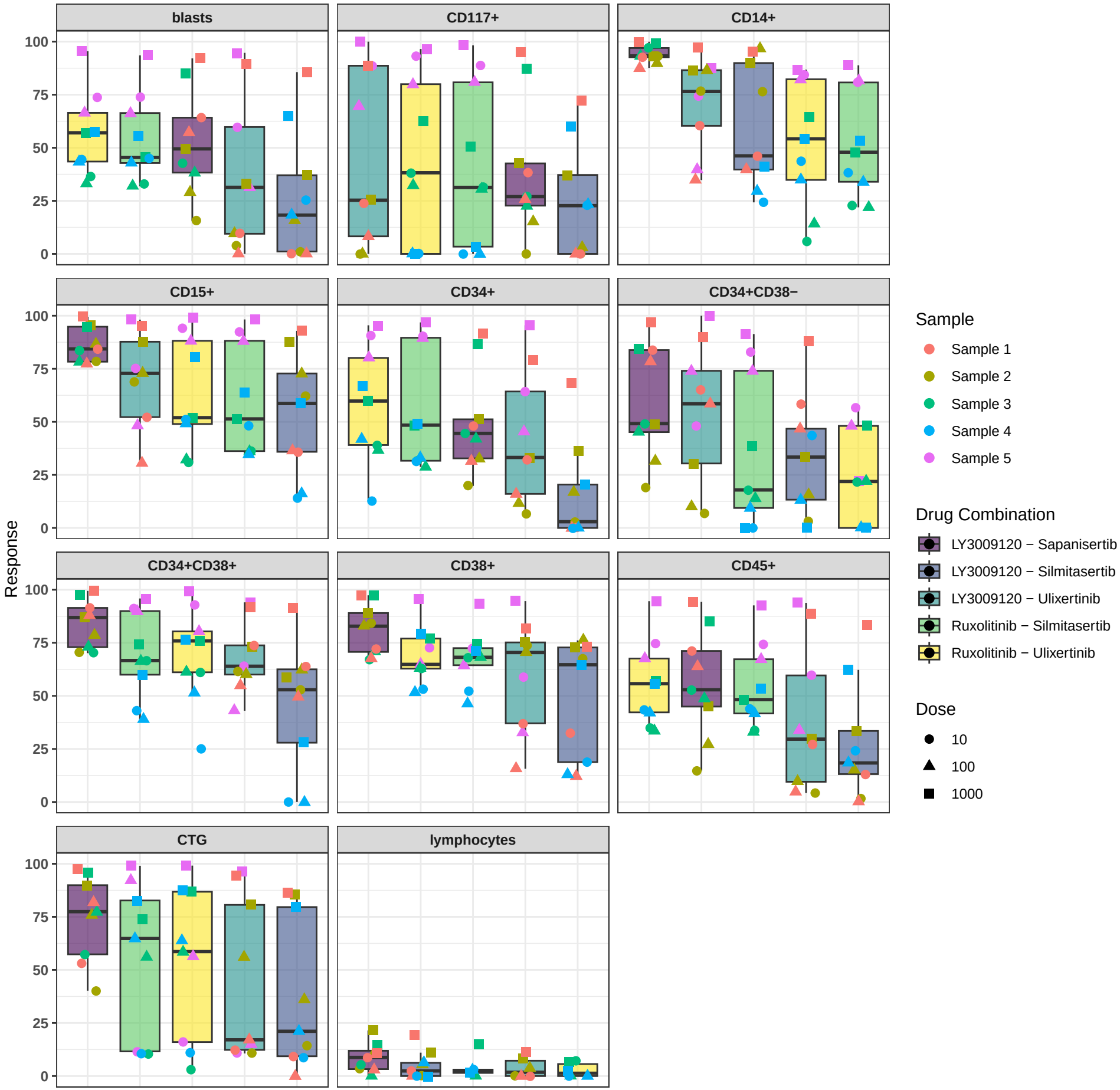
blasts
CD117+
CD14+
CD15+
CD34+
CD34+CD38−
CD34+CD38+
CD38+
CD45+
CTG
lymphocytes
Response
0
25
50
75
100
Sample
Sample 1
Sample 2
Sample 3
Sample 4
Sample 5
Drug Combination
LY3009120 − Sapanisertib
LY3009120 − Silmitasertib
LY3009120 − Ulixertinib
Ruxolitinib − Silmitasertib
Ruxolitinib − Ulixertinib
Dose
10
100
1000

Figure 6

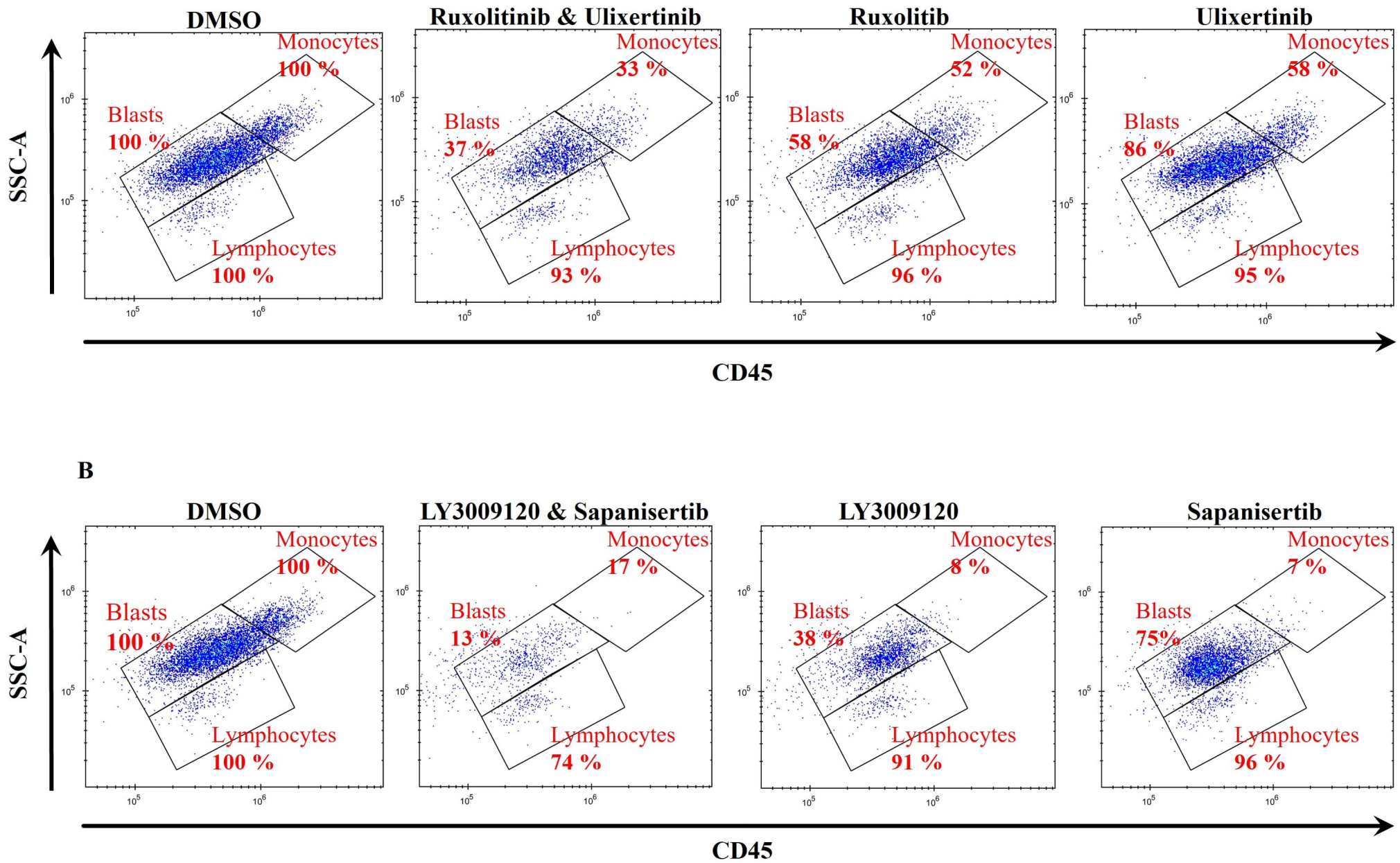
A
DMSO
Monocytes
100 %
Blasts
100 %
Lymphocytes
100 %
Ruxolitinib & Ulixertinib
Monocytes
33 %
Blasts
37 %
Lymphocytes
93 %
Ruxolitib
Monocytes
52 %
Blasts
58 %
Lymphocytes
96 %
Ulixertinib
Monocytes
58 %
Blasts
86 %
Lymphocytes
95 %
SSC-A
CD45
B
DMSO
Monocytes
100 %
Blasts
100 %
Lymphocytes
100 %
LY3009120 & Sapanisertib
Monocytes
17 %
Blasts
13 %
Lymphocytes
74 %
LY3009120
Monocytes
8 %
Blasts
38 %
Lymphocytes
91 %
Sapanisertib
Monocytes
7 %
Blasts
75%
Lymphocytes
96 %
SSC-A
CD45

Figure 7

A)

	AML sample	1	2	3	4	5
Single drugs	Ruxolitinib			19.40	23.40	48.00
	Silmitasertib	7.40	1.70	2.30	3.90	5.00
	Ulixertinib	12.90	0.20	5.80	5.50	10.40
	LY3009120	17.10	8.50	13.10	15.40	38.70
	Sapanisertib	44.60	0.00	9.50		
Drug combinations	Sapa_LY30	92.10	49.50	85.00		
	Ulix- Ruxo			57.10	80.30	95.50
	Silm-Ruxo			45.50	63.80	93.50
	Silm-LY30	85.70	37.10		60.00	
	Ulix-LY30	89.60	33.10			94.70
Drug combinations	Sapa_LY30	12.89	25.51	16.55		
	Ulix- Ruxo			6.67	2.60	70.84
	Silm-Ruxo			14.76	1.55	59.68
	Silm-LY30	19.27	11.02		-14.02	
	Ulix-LY30	11.17	8.44			60.92
Blast	Sapa_LY30	9.35	15.60	19.06		
	Ulix- Ruxo			18.14	14.67	7.34
	Silm-Ruxo			5.88	0.00	4.92
	Silm-LY30	1.14	4.58		0.93	
	Ulix-LY30	4.47	0.62			6.27
Lymphocyte	Sapa_LY30	6.38	12.89	6.03		
	Ulix- Ruxo			6.35	2.59	10.70
	Silm-Ruxo			14.75	1.54	-2.57
	Silm-LY30	12.74	12.75		0.00	
	Ulix-LY30	4.64	4.64			11.61
Molecular Profiling	Disease Stage	Rf	R	D	D	R
	GATA2					
	DNMT3A					
	NPM1					
	FLT3					
	TET2					
	NRAS					
	SMC3					
	SRSF2					
	KMT2A					
	CROCC					
	FAB subtype	M5		M5	M2	M5
	Blast Ratio	0.16	0.76	0.76	0.94	0.89

DSS (FC Blast): 0 | 20 | 40 | 60; N/A

%Apoptotic(FC Blast): 0 | 40 | 80 | 100; N/A

%Apoptotic(FC Lymphocytes): 0 | 40 | 80 | 100; N/A

HSA(Synergy): 0 | 5 | 10 | 20; N/A

HSA(Synergy): 0 | 5 | 10 | 20; N/A

Non-mutated; Mutated; N/A

B)

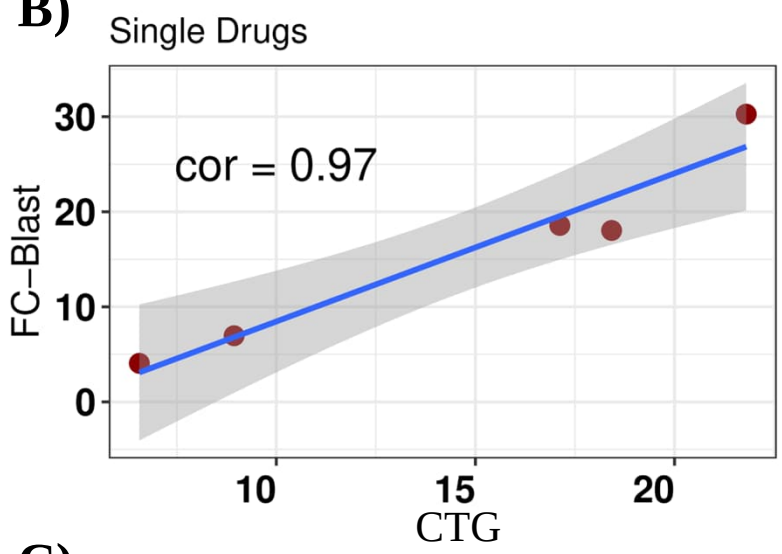

C)

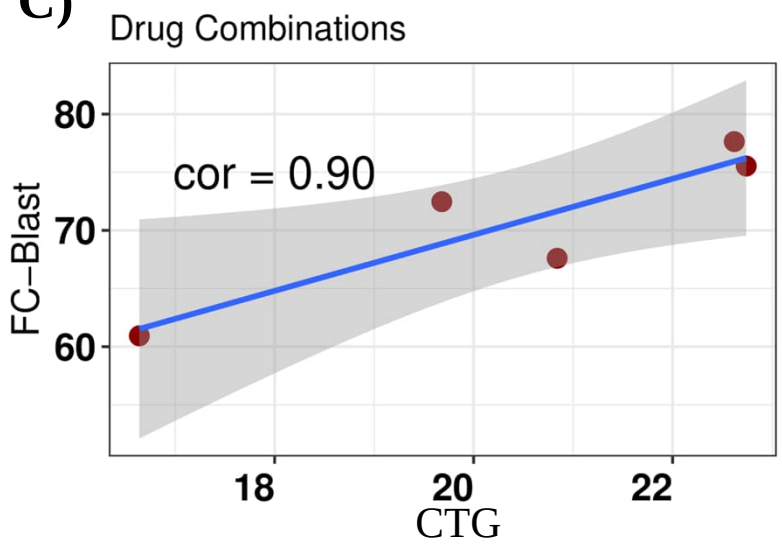

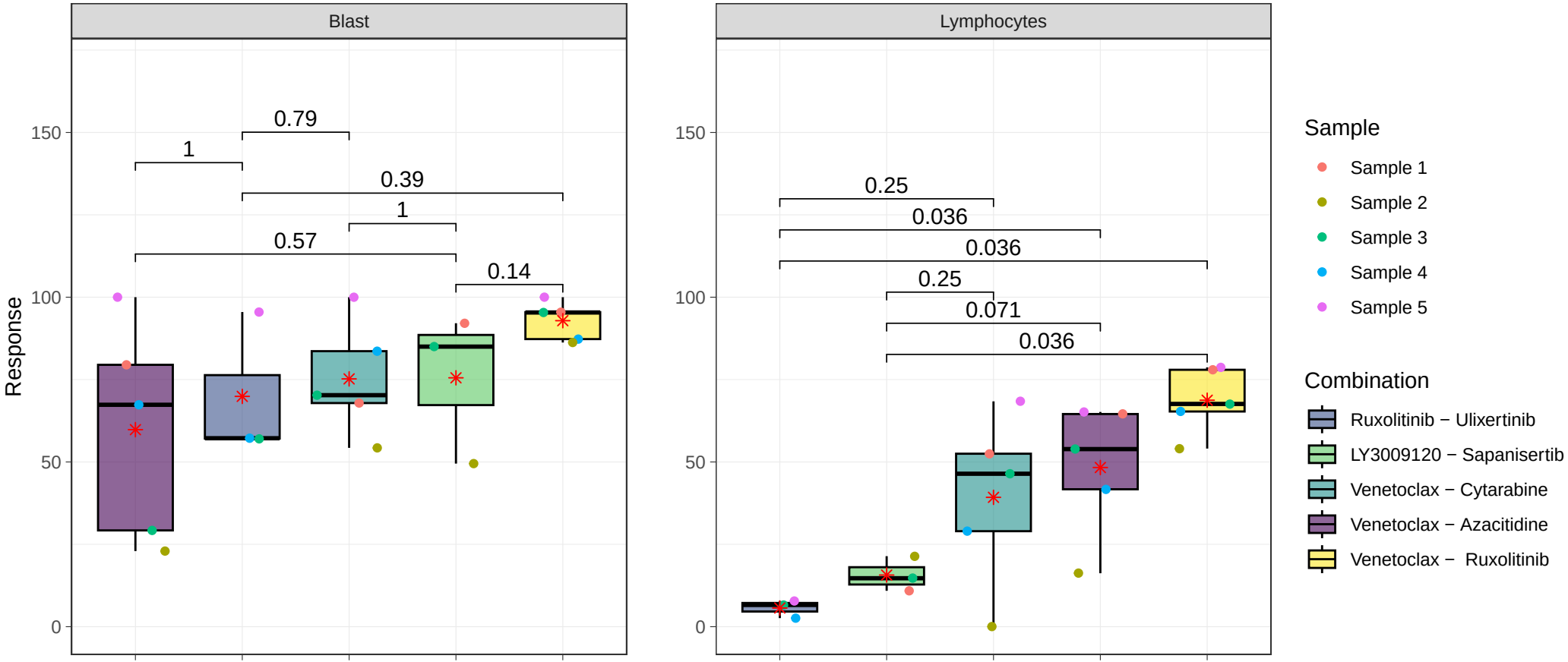
Blast
Lymphocytes
Response
150
100
50
0
1
0.79
0.39
1
0.57
0.14
0.25
0.036
0.036
0.25
0.071
0.036
Sample
Sample 1
Sample 2
Sample 3
Sample 4
Sample 5
Combination
Ruxolitinib − Ulixertinib
LY3009120 − Sapanisertib
Venetoclax − Cytarabine
Venetoclax − Azacitidine
Venetoclax − Ruxolitinib

Table 1. The selected chemical compounds from two clusters of drugs in the drug similarity network.

Cluster 1	Cluster 2
LY3009120 (LY30)	Teniposide (Teni)
Ruxolitinib (Ruxo)	Silmitasertib (Silm)
Birabresib (Bira)	Ulixertinib (Ulix)
Plicamycin (Plic)	Sapanisertib (Sapa)

Table 1. Selected drug combinations sorted by synergy scoring functions. Highlighted in green (inter-cluster), yellow (intra-cluster 1), and purple (intra-cluster 2). Inh stands for the average of inhibition of drug combinations on dosages, ZIP, hsa, bliss, and loewe are synergy scorings and CR is the combination ratio.

Drug Combinations	Inh	ZIP	hsa	bliss	loewe	CR
LY3009120 , Silmitasertib						
Ulixertinib , Ruxolitinib						
Silmitasertib , Ruxolitinib						
Sapanisertib , LY3009120						
Ulixertinib , LY3009120						
Ulixertinib , Plicamycin						
Birabresib , Ulixertinib						
Birabresib , Teniposide						
LY3009120 , Ruxolitinib						
Sapanisertib , Ulixertinib						
Ulixertinib , Silmitasertib						